LA-UR- 97-2384

CONF-970706--7

Approved for public release; distribution is unlimited.

Title: SYCNCHRO-BALLISTIC RECORDING OF DETONATION PHENOMENA

Author(s): Robert R. Critchfield, DX-4
Blaine W Asay, DX-2
John B. Bdzil, DX-1
William C. Davis, DX-1
Eric N. Ferm, DX-3
Deanne J. Idar, DX-2

Submitted to: The Int'l Society for Optical Engineering
P.O. Box 10
Bellingham, Washington 98227-0010

International Symposium on Optical Science, Engineering and Instrumentation
San Diego, CA 7/27/97 - 8/1/97
(SPIE paper #3173A 14)

Los Alamos
NATIONAL LABORATORY

Synchro-ballistic recording of detonation phenomena

R. R. Critchfield, B. W Asay, J. B. Bdzil, W. C. Davis, E. N. Ferm, D. J. Idar

Los Alamos National Laboratory, Los Alamos, NM 87545

ABSTRACT

Synchro-ballistic use of rotating-mirror streak cameras allows for detailed recording of high-speed events of known velocity and direction. After an introduction to the synchro-ballistic technique, this paper details two diverse applications of the technique as applied in the field of high-explosives research.

In the first series of experiments detonation-front shape is recorded as the arriving detonation shock wave tilts an obliquely mounted mirror, causing reflected light to be deflected from the imaging lens. These tests were conducted for the purpose of calibrating and confirming the asymptotic Detonation Shock Dynamics (DSD) theory of Bdzil and Stewart[1]. The phase velocities of the events range from ten to thirty millimeters per microsecond. Optical magnification is set for optimal use of the film's spatial dimension and the phase velocity is adjusted to provide synchronization at the camera's maximum writing speed. Initial calibration of the technique is undertaken using a cylindrical HE geometry over a range of charge diameters and of sufficient length-to-diameter ratio to insure a stable detonation wave. The final experiment utilizes an arc-shaped explosive charge, resulting in an asymmetric detonation-front record.

The second series of experiments consists of photographing a shaped-charge jet having a velocity range of two to nine millimeters per microsecond. To accommodate the range of velocities it is necessary to fire several tests, each synchronized to a different section of the jet. The experimental apparatus consists of a vacuum chamber to preclude atmospheric ablation of the jet tip with shocked-argon back lighting to produce a shadow-graph image.

Keywords: synchro, ballistic, streak, smear, shaped charge, jet, explosive, detonation, hypersonic, photography

1. INTRODUCTION

One of the oldest (and most easily visualized) examples of the synchro-ballistic technique can be found in the traditional finish-line camera used in horse racing, depicted here as Figure 1. The camera lens images the finish line (a plane in space) onto a narrow, vertical, slit opening inside the camera. Film is transported horizontally immediately behind the slit and, as a horse traverses that plane in space, the image of the horse traverses the slit in the same direction and at the same speed as

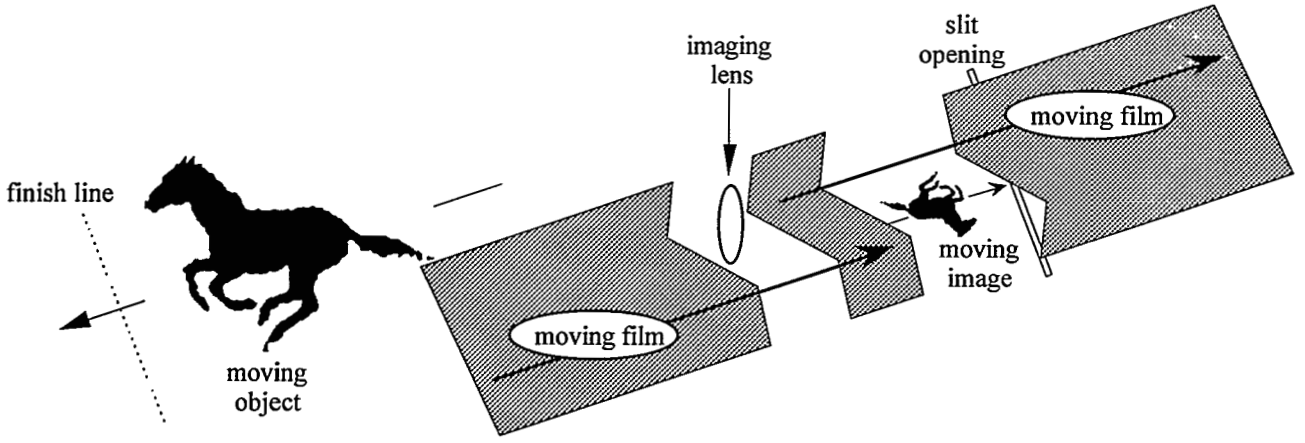

Figure 1 - Diagram of race track finish-line camera.

the moving film. The light can reach the film only through the slit opening. The resulting film record is not a true snapshot because the leading and trailing edges of the horse's image are recorded on film at different times, i.e. the record is x,t rather than x,y. Hypothetically, a horse's gait might be such that it always raises and lowers its head and tail in unison as it runs. One could conceivably record a synchro-ballistic image of that horse with its tail up and its head down, creating a false x,y impression. And, since the horse is changing shape during the exposure, the entire image would be distorted. Of course in determining the winner of a photo-finish race such fine points do not pose a problem at the race track. An object that is not changing shape can be captured synchro-ballistically without distortion; but even a distorted image can be corrected if one knows enough about the change in shape that is occurring during the record's acquisition.

In the above example, were the film to be moving significantly faster than the horse's image, the resulting picture would be stretched out along the horizontal axis; that is to say the image captured on film might resemble a horse less than a cross between a horse and a dachshund. If the film were moving noticeably slower than the image, the film record would be compressed along the horizontal axis and the horse's photograph might more closely resemble that of a giraffe than of a normal horse. If both the horse's image and the film were to be moving at the same speed they would be synchronized and the resulting photo would have true horizontal proportions. In the real world one cannot achieve perfect synchronization. Some amount of distortion is to be anticipated and that fact needs to be taken into consideration when analyzing results.

The fastest of horses can only travel a few tens of feet per second and the image of a racetrack finish line must be demagnified to fit on film of normal proportions. This results in an image speed on the order of one foot per second. Transporting film at that speed is not a problem for the simplest of film transport mechanisms. High-speed transports are available that can move film at a few hundred feet per second and even supersonic events can be synchronized with such a camera if the image is demagnified sufficiently. A common example of such high-speed transport can be found in the cameras used in sled-track tests. But at hypersonic speeds, and with little or no demagnification, only stationary film and a moving slit image can allow the synchro-ballistic technique to succeed. This is readily accomplished with a rotating-mirror streak camera. In this case, the image of the plane in space is superimposed on the camera's slit and that composite image is relayed to film by way of the rotating mirror. For proper synchronization, the composite slit image must be swept along the film in a direction opposite that of the image motion. This maintains the same lack of relative motion between the stationary film and the moving subject's image as was the case when the film was moving and the slit was stationary.

Regardless of speed, if synchronization is achieved there will be no blur. This is true because there is no relative movement between image and film and the slit serves only to control exposure. Lack of synchronization produces both distortion and blur. With ample illumination, however, the blur can be minimized by utilizing the smallest possible slit width.

2. DETONATION SHOCK DYNAMICS (DSD) EXPERIMENTS

To record curvature of the detonation front in PBX 9502 explosive, two explosive geometries were employed. The first, and simplest, geometry was that of a right circular cylinder and tests were conducted on cylinders of 10, 12, 18 and 50 millimeters diameter. These cylinders were dubbed "rate" sticks because external electrical pins were employed along the outside surface of the explosive to measure detonation velocity and to confirm that the detonation front was stable. The cylindrical explosive assemblies used had sufficient length-to-diameter ratio to establish a stable detonation front. To help achieve that detonation-front stability the smaller sticks were end initiated with a point-source detonation while the 50 mm rate stick was end initiated with an explosive plane-wave lens. Planar initiation of the largest rate stick was chosen because its detonation front curvature, once stabilized, would be far less than that of the smaller specimens.

The second geometry was that of an explosive cylindrical arc segment of 135° arc displacement. The arc segment was also initiated by a plane-wave lens and was of sufficient height along the cylindrical axis to keep top and bottom edge effects from perturbing the detonation front at mid-height, where the image was recorded.

In both geometries, the physical dimensions relating to the experimental data were accurately measured with an optical cathetometer and all tests were conducted at the same carefully controlled temperature (74° C.) The explosive pieces used in the DSD experiments were machined from a single highly uniform pressing of PBX 9502 explosive of 1.84 g/cm^3 density. The 70 millimeter film camera used to photograph these experiments was of Winslow/Davis design[2] and was built in-house.

2.1. Rate-stick tests

The camera's optical axis relative to the smallest (10 mm) rate-stick geometry is illustrated in Figure 2, which shows that

light passing through a narrow aperture of an explosively driven argon light source reflects off the terminal end of the experiment before being collected by the camera's imaging lens and relayed to the horizontally situated slit. The light reflects off the experiment via a tilting mirror. This relationship between light source, tilting mirror and camera slit was

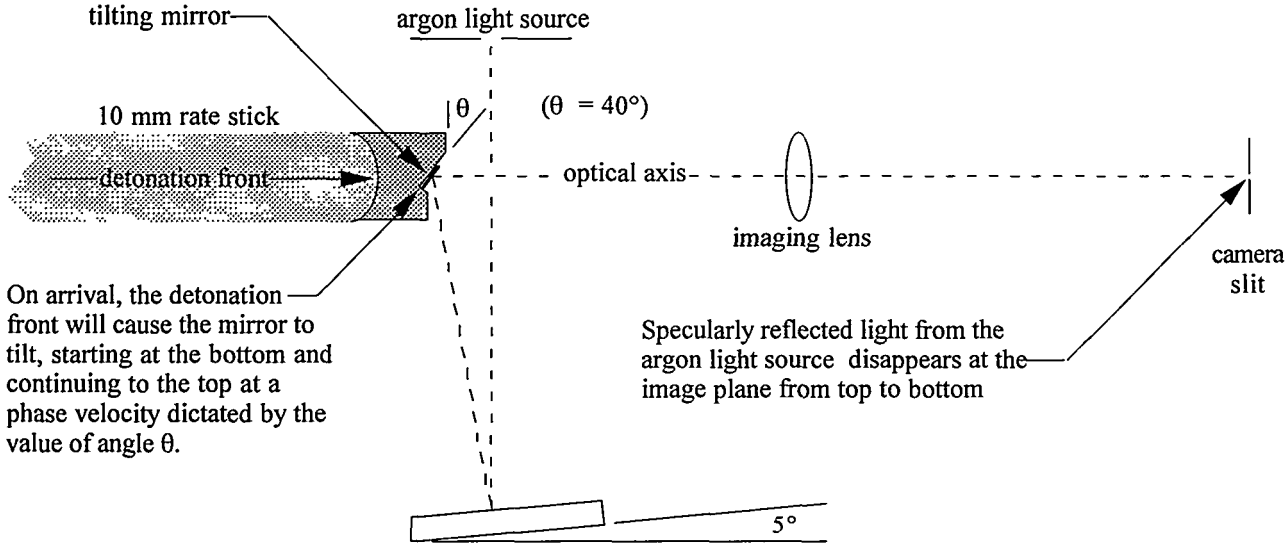

Figure 2 - Diagram of the light path for the 10 mm rate stick experiment.

common to all tests in the DSD series. The mirror is an aluminized pattern deposited on a glass slide and it is attached with the aluminized surface in direct contact with the explosive. The camera's view of the tilting mirror is represented in Figure 3.

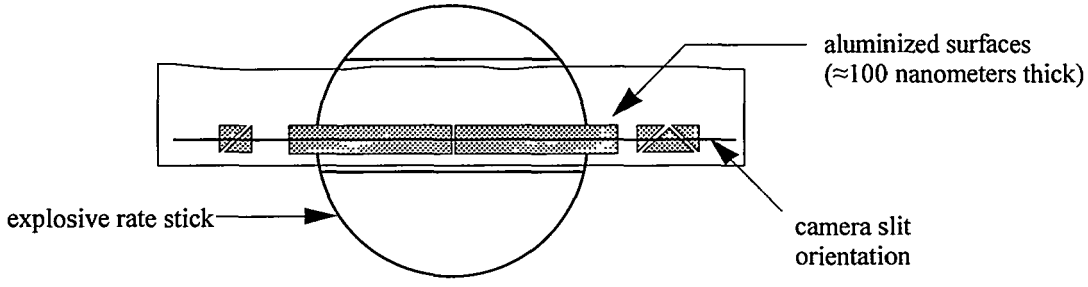

Figure 3 - Diagram of the tilting mirror, illustrating rectangular mirror patterns with fiducial breaks.

With the long axes of the light-source aperture, the mirror surface and the camera's slit all parallel, and the mirror surface focused upon the slit, the detonation front arrives and the tilting motion of the mirror surface promptly deflects the light from the camera's slit. So great is the shock pressure acting on the aluminized surface that that surface distorts and bends before the front surface of the glass slide is affected in any way. Additionally, the apparent disappearance of the specularly reflected light from bottom to top of the mirror surface is recorded synchro-ballistically to optimize the image sharpness. On the dynamic film record, the break in the middle of the aluminized surface will mark the experiment's center, the outboard mirrored surfaces mark right versus left, the 45° breaks verify proper alignment to the slit and the four rectangles define scale.

In contrast to Figure 2, the geometry illustrated in Figure 4 is that of the 50 millimeter diameter rate stick. The marked difference in mirror angle is to accommodate the reduced magnification, in this largest experiment of the series, by increasing the vertical phase velocity at the mirror surface. Camera slit length, and therefore, image size was fixed and maximum slit-image sweep speed (15.76 mm/μs) was used throughout all experiments, to optimize resolution. This resulted in a magnification range

of 0.33 (50 mm rate stick) to 1.75 (10 mm rate stick.) For proper ballistic synchronization, throughout that range of magnification, the angle (θ) of mirror tilt from the vertical plane is simply:

$$\tan\theta = \frac{\text{magnification x detonation velocity}}{\text{slit image writing speed}}$$

Given a detonation velocity of 7.55 mm/μs, the above equation defines the range of mirror tilt as being from 9° to 40° off vertical.

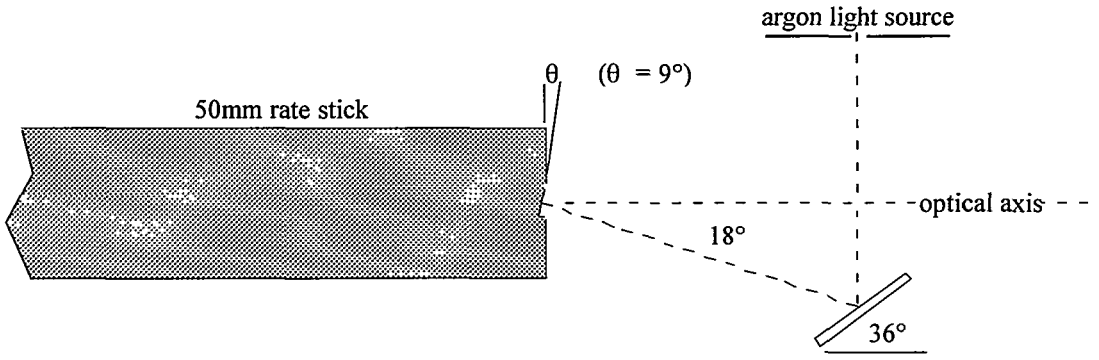

Figure 4 - Diagram of light path for the 50 mm rate stick experiment, illustrating the extreme phase angle needed to maintain synchronization at this, the lowest, image magnification used.

The center portion of the film record (not including data from the outboard mirror sections) for the 50 mm rate stick is shown in Figure 5, which is a positive image of the record with the slit sweeping from top to bottom. Prior to arrival of the detonation front, the camera's slit is bathed in light. The first reduction in exposure is coincident with the tilting of the aluminized mirror surface and the second reduction is a result of the second (outer) surface of the glass slide tilting and deflecting the remaining specularly reflected light from the camera's slit. Since this record was acquired at the lowest magnification it shows far more curvature than that of the detonation front itself. The leading edge data were subsequently digitized and analyzed to correct for the effects of mirror angle, magnification and sweep speed.

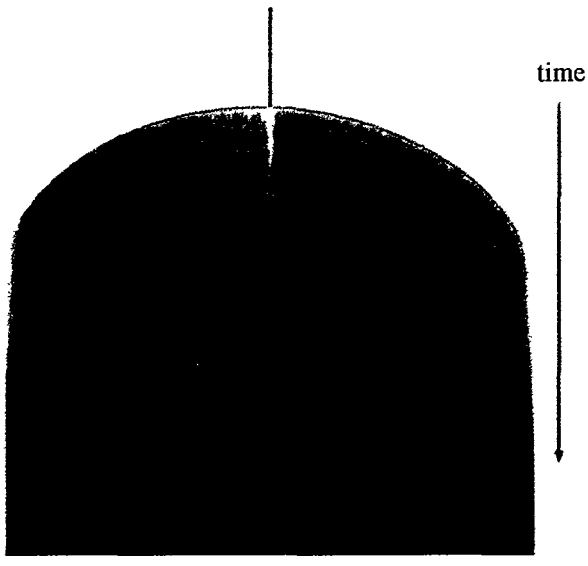

Figure 5 - Digital scan of 50 mm rate stick record

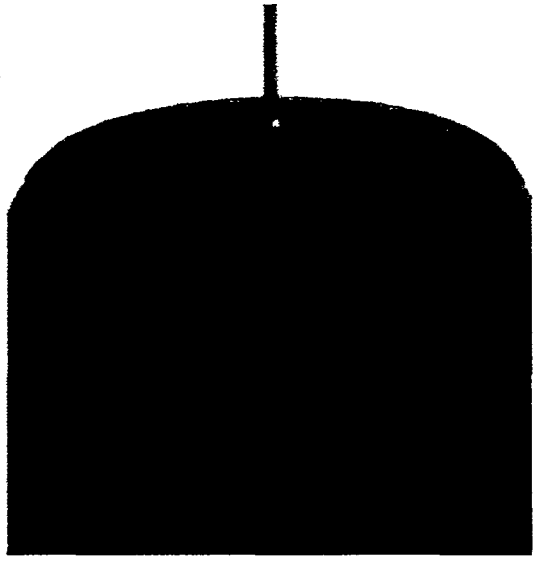

Figure 6 - Digital scan of 10 mm rate stick record.

Figure 6 is the film record from the 10 mm rate stick. Featuring the highest magnification, the leading edge has much less curvature than the actual detonation front. Digital analysis was again employed to convert the tilting mirror data into that of the detonation front.

In these experiments, digital correction is necessary only because we are recording an image in order to deduce the shape of the event that caused that image. For image clarity, synchronization was keyed to the tilting mirror's vertical phase velocity rather than to the detonation velocity. To record the actual shape of the detonation front on film one could set θ equal to 45° for all tests ($\tan \theta = 1$) and adjust the writing speed of the camera to equal the product of detonation velocity times image magnification. The image, however, would lack optimum temporal resolution at the slower camera speeds needed for proper synchronization and hydrodynamic interaction between the tilting mirror and the detonation shock actually limits the value of θ to 40° or less.

Figure 7 is the resultant plot of the four detonation front shapes from the rate stick tests.

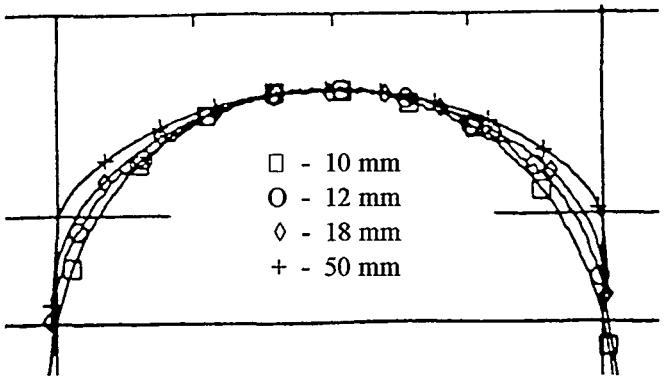

Figure 7 - Unsymmetrized shock loci of 10, 12, 18 and 50 mm diameter rate sticks, normalized for scale.

2.2. Arc segment test

A top-view diagram of the explosive cylindrical arc segment is shown here as Figure 8. Because the detonation front in this experiment was asymmetric, it was necessary to employ two sets of electrical "pins," one set each on the outside and inside surfaces of the arc, to verify that the detonation-front shape was stable.

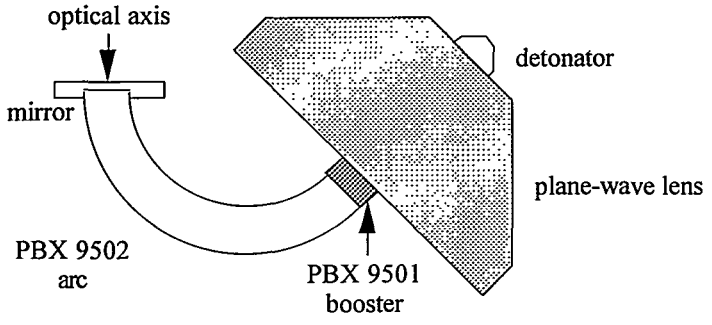

Figure 8 - Diagram of PBX 9502 explosive arc segment, as viewed from above.

Figure 9 is the film record from the arc-segment experiment, sweeping from left to right and with the inside radius at the bottom of the illustration. While the several rate stick tests served to calibrate the DSD model with a simple detonation-front geometry, the data from this final test in the series very closely matched the shape predicted by the Bdzil/Stewart DSD theory in this more demanding geometry and served to validate the theory's algorithm.

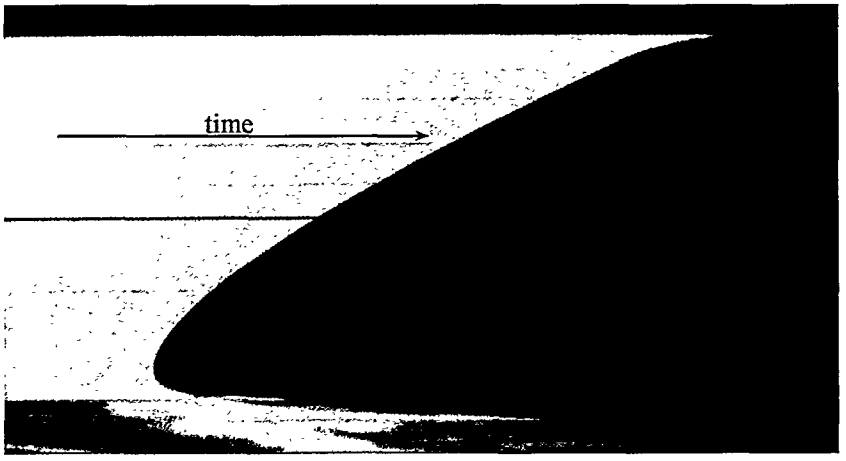

Figure 9 - Digitally scanned synchro-ballistic film record of cylindrical arc-segment test.

The images in Figures 5, 6 and 9 could have been collected in a simpler fashion (e.g. a simple flash gap), but synchro-ballistic recording of the tilting mirror gives a much sharper and more detailed image than that achieved by alternative methods. This is because the normal slit widths (50 - 100 microns) are significantly greater than the least resolved distance the camera is capable of measuring (60 line pairs per millimeter).[2] It is worth pointing out that the effort needed to employ this technique will probably be well spent only if critical measurement requirements or a lack of subject brilliance (i.e. the need to use a very wide slit) dictate its use.

3. VIPER SHAPED-CHARGE JET EXPERIMENTS

Though the peak velocity of the Viper shaped-charge jet is an order of magnitude greater than that of a high-velocity rifle bullet, it is an easier experiment to conceptualize than the previous (DSD) example. Flash radiographs of the jets show them to resemble arrows cast from a bow, albeit at a velocity two orders of magnitude greater than their fletched counterparts. A dynamic feature of the jet is that it has a significant velocity gradient across its length. It is literally pulling itself apart in flight and will ultimately particulate. The goal of this series of tests was to measure diameter variations along the profile of the jet stem prior to particulation. Due to the velocity gradient of the subject and the constant writing speed of the camera, numerous experiments need to be conducted to collect optimally synchronized data for the full visible length of the jet. For the purpose of this paper only a few tests will be illustrated.

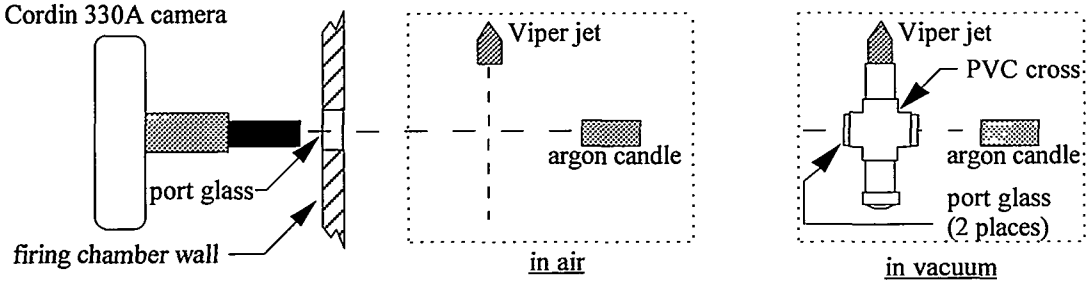

Figure 10 - Diagram of test layouts for the Viper jet experiments.

Figure 10 illustrates that the jet need only pass through the object plane of the imaging lens at right angles to both the optical axis and the slit, and at the point of focus, to be properly recorded on film. Of course, the arrival of the jet, the firing of the back-lighting charge and the sweep of the slit image across the film must also be accurately timed. The camera used in this series of tests was a Cordin™ model 330A, chosen for its relatively long (430 millimeters) streak record.

With an initial image magnification of one-third and a sweep speed of 3 mm/μs, the Cordin camera was synchronized at the tip velocity of the jet (9 mm/μs). The record shown as Figure 11 is that of the Viper jet fired in air, traveling left to right. The opaque mass obscuring the jet body is the result of tip ablation as the jet penetrates the atmosphere. This record was purposefully over-exposed in an effort to see through the obscuration. At the far left of Figure 11 the jet stem is barely visible. Even there, however, the jet's image is distorted by the heated and turbulent atmosphere surrounding the jet body.

Figure 11 - Digitally scanned synchro-ballistic film record of Viper jet fired in air.

A subsequent experiment fired in a helium atmosphere showed little change, so it was determined that the tests would have to be performed in a very thin atmosphere, or rough vacuum. To maintain the experiment's affordability, a vacuum chamber was constructed of 4-inch PVC pipe and fittings. A cross-section diagram of the PVC assembly is shown as Figure 12.

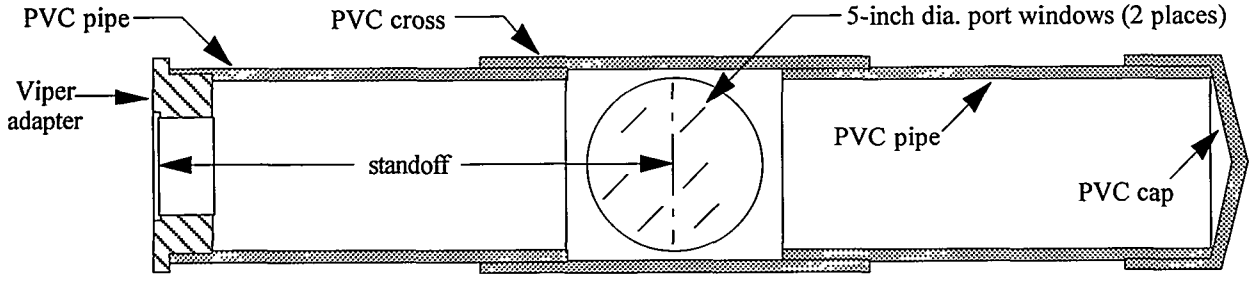

Figure 12 - Cross-section of PVC vacuum assembly.

To facilitate quick and accurate fielding of the experiment, the pipe section defining the Viper standoff was first glued to the cross which was then chucked in a lathe with that axis of the cross on lathe center. A counterbore was turned in the end of the pipe to accept the machined Viper adapter, establishing precise standoff and aiming of the Viper assembly. The axis of the PVC cross that is normal to the page in Figure 12 then had its ends counterbored square to the jet axis to accept 5-inch diameter BK-7 port windows on the camera's optical axis. Not shown in the diagram, a hole and counterbore were machined into the top of the assembly for a vacuum flange that would also accept a focusing and alignment jig, for optical setup prior to hooking up the vacuum line and evacuating the air from the assembly. With the second pipe section and cap in place, the Viper jet's copper liner formed the final component of the vacuum assembly. After an initial twenty-four hour purge to out-gas the PVC, the assembly was quickly and easily set up for firing at a rough vacuum of 100 microns or better. A repeat of the test that produced the image in Figure 11 was fired in the vacuum chamber and the result is shown here as Figure 13.

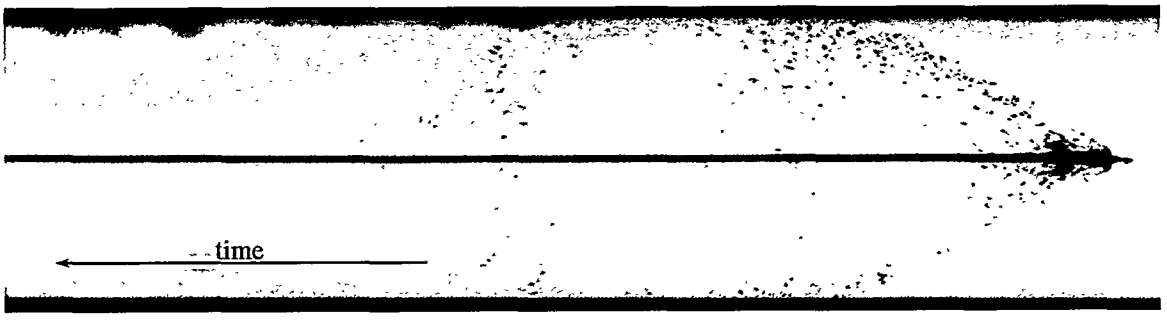

Figure 13 - Digitally scanned synchro-ballistic film record of Viper jet fired in a vacuum. Synchronization is at the speed of the jet tip.

The characteristic shape of the jet tip is quite the same, in Figure 13, as when imaged with flash radiography, but much finer detail is visible in the synchro-ballistic photograph. The effects of changing the synchronization can be readily seen in Figure 14, where the record is synchronized in the left half of the illustration. This test was conducted at twice the image magnification of the previous two, but with all other parameters remaining the same. Just as with the small rate stick and the hypothetical horse's image that resembled a giraffe, the image of the jet tip in Figure 14 is compressed horizontally with the bow wave much less acute in angle. Farther back along the jet stem where the speeds were synchronized, however, the image is clear and proportional (horizontally and vertically) to the object being photographed.

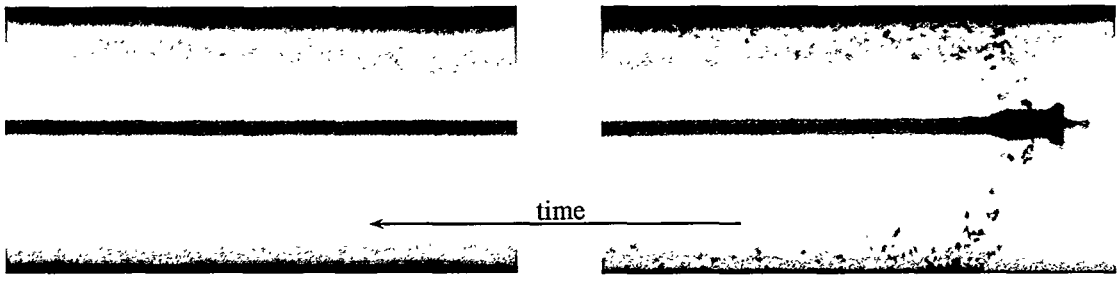

Figure 14 - Digitally scanned synchro-ballistic film record of Viper jet fired in a vacuum. In the original record, the jet body that is missing from the middle of this illustration is nearly the same length as these two images combined. The point of synchronization is near the left edge of the illustration, at one-half tip velocity.

4. CONCLUSION

Synchro-ballistic photography has been described and two examples of utilizing the technique for the recording of hypervelocity events of explosive origin have been detailed. In the DSD example the synchro-ballistic technique provided a much enhanced record, when compared to more conventional smear camera techniques. The Viper-jet results illustrate that the technique can be useful in capturing an object in stable flight, along an approximate straight line, at virtually any velocity.

5. ACKNOWLEDGMENTS

Firing site leaders H. H. Harry, V. M. Sandoval and L. E. Viramontes provided invaluable assistance in fielding these experiments. K. Kasman and G. Robinson did most of the machining and made significant contributions to the design of the experimental apparatuses. This work was performed under the auspices of the United States Department of Energy.

6. REFERENCES

1. T Aslam, J. Bdzil, D. Stewart; "Level set methods applied to modeling detonation shock dynamics;" *Journal of Computational Physics*; vol. **126**, article no. 0145; pp. 390-409 (1996).

2. O. Winslow, W. Davis; "Rotating mirror streak camera with an optional image intensifier camera back;" *High Speed Photography, Videography and Photonics V*; Vol. 832, pp. 96-100; SPIE (1987).